X002

Seismic Scanning Tunneling Macroscope - Elastic Simulations and Arizona Mine Test

S.M. Hanafy* (King Abdullah University of Science & Technology) & G.T. Schuster (King Abdullah University of Science & Technology)

SUMMARY

Elastic seismic simulations and field data tests are used to validate the theory of a seismic scanning tunneling macroscope (SSTM). For nearfield elastic simulation, the SSTM results show superresolution to be better than $\lambda/8$ if the only scattered data are used as input data. If the direct P and S waves are muted then the resolution of the scatterer locations are within about $\lambda/5$. Seismic data collected in an Arizona tunnel showed a superresolution limit of at least $\lambda/19$. These test results are consistent with the theory of the SSTM and suggest that the SSTM can be a tool used by geophysicists as a probe for near-field scatterers.

Introduction

The theory of the seismic scanning tunneling macroscope (SSTM) was recently presented by Schuster et al. (2012); they showed that super-resolution images of near-field scatterers can be computed from far-field data if the scatterers are subwavelength in dimension and time reverse mirrors (TRM) are used for the imaging operation (Fink, 2008). We now present results with elastic simulations and a field data test in Arizona that validate the super-resolution properties of the SSTM.

Synthetic Elastic Data Tests

Synthetic elastic data are used for testing sub-wavelength resolution of near-field scatterers by TRM, where a finite-difference solution to the wave equation is used to generate elastic data (Figure 1a) for the synthetic 7-scatterer model shown in Figure 1b. The time reverse mirrors (TRM) equation (Fink 2008) is defined as

$$\boldsymbol{s'}\epsilon B_s \quad m(\boldsymbol{s'}) = \sum_{B_g} d(\boldsymbol{g},t|\boldsymbol{s},0)^{Scatt.} d(\boldsymbol{g},t|\boldsymbol{s'},0)^{extrapolator} \tag{1}$$

and will be used to obtain the TRM profile $m(\mathbf{s'})$. Here, $d(\boldsymbol{g},t|\boldsymbol{s},0)^{Scatt.}$ represents data for a source at $\mathbf{s}$ and a geophone at $\boldsymbol{g}$; the geophone locations are along the line $\boldsymbol{B_g}$ at the free surface. In this formula, the input scattered data consist of the scattered energy recorded at $\boldsymbol{g} \in \boldsymbol{B_g}$ excited by a single source at $\mathbf{s} \in B_s$, and the output of this equation is the TRM profile $m(\mathbf{s'})$ for different trial source points $\mathbf{s'}$. A sample CSG with a source at (x,z)=(48.8, 36) m is shown in Figure 1a, where the source is a z-component point displacement with a Ricker wavelet peaked at 100-Hz.
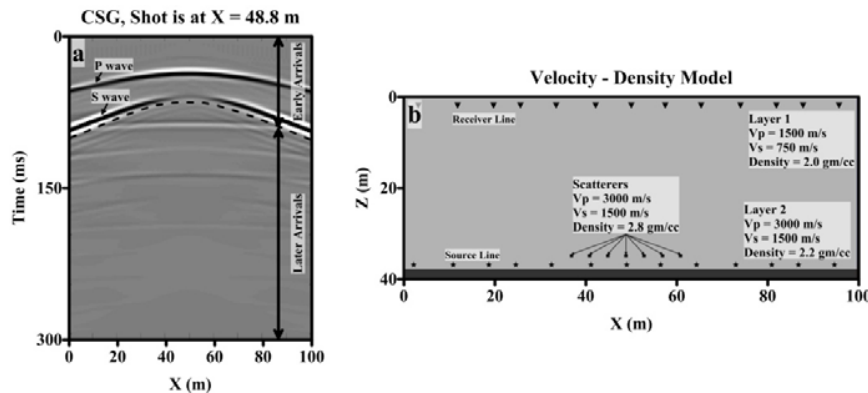

Figure 1 *a) A common shot gather (CSG) containing 181 traces with a 0.2 m trace interval and a shot location at x=48.8 m. The dashed line in the CSG is the boundary between early (direct-only) arrivals and later (scattered-only) arrivals. b) Velocity model used to generate the synthetic CSGs. V_P, V_S, and density values are shown on the Figure. Here, 7 scatterer points are added at a depth of 36 m from ground surface.*

The TRM profile is computed by zero-lag correlation of the trace $d(\mathbf{g},t|\mathbf{s'},0)^{extrapolator}$ with the trace $d(\mathbf{g},t|\mathbf{s},0)^{scatt.}$ and summing over geophone positions at $\mathbf{g}$ to get $m(\mathbf{s'})$, the TRM profile for the actual source at $\mathbf{s}$. There are two different procedures for isolating scattered events from the direct waves.

1. Mute the early arrivals to eliminate the direct arrivals and retain the near-field scattered arrivals. In this case, the early arrivals are defined as the energy above the dashed line in Figure 1a, and the remaining part defines the later scattered arrivals. Implicit in this windowing is the assumption that the near-field scattered energy is reverberating between the scatterers and the lower reflector. Figure 2a shows the TRM profile for the early-arrival energy where later arrivals are muted, while Figure 2b shows the thinner TRM profile for the scattered-only energy. This increase in resolution is due to the near-field scattering. Cross

sections along (A-B) in Figure 2a-b are shown in Figure 2d and represent the TRM profiles for the true source at X=48.8 m. If the horizontal spatial resolution limit is defined to be the width of the main lobe at half the maximum amplitude, and the minimum wavelength is λ_{min} = V_p/Frequency=1500/100=15 m, then the direct-only resolution is Δx^{direct} = 19.2 m = 1.3* λ_{min} and the scattered-only resolution is $\Delta x^{scatt.}$ = 3.6 m = $\frac{\lambda_{min}}{4.2}$ as shown in Fig. 2d.

2. Compute the CSGs for the velocity model without scatterers, compute the CSGs with scatterers, and then subtract the two data sets. This differenced CSG will be referred to as the "differenced" Green's function. Figure 2c shows the TRM profiles for the differenced Green's function. The cross-section of the TRM profile in Figure 2c is plotted in Figure 2d and shows a resolution of 1.8 m = $\frac{\lambda_{min}}{8.3}$.

The elastic simulations results confirm that TRM profiles with super-resolution can be obtained from far-field scattered records. Muting the early arrivals is sufficient for obtaining super-resolution TRM profiles in this example, but differencing seismograms is more effective.
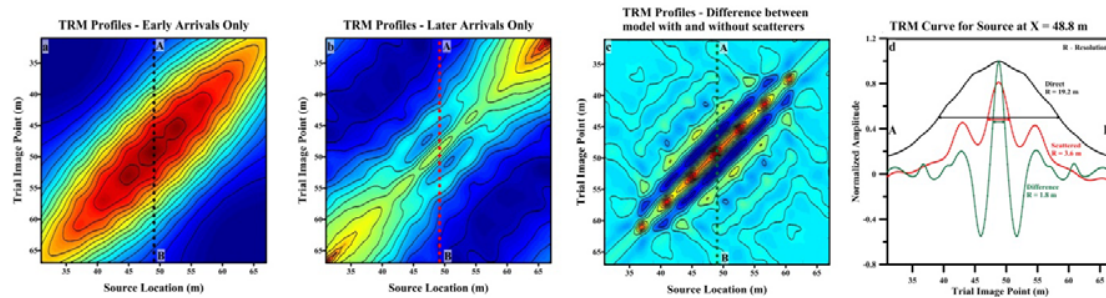

Figure 2 *TRM profiles m(s') for different source and trial source locations calculated from traces that exclusively contain a) direct waves b) later arrivals, and c) scattered waves. The source location is at X=48.8 m. d) Cross sections (A-B) taken at the source location X=48.8 m for the three panels (a, b, and c). Hotter colors correspond to larger TRM amplitudes*

Tucson Field Data Tests

The field data test is a controlled-source seismic experiment (Cao et al., 2011) in a mine near Tucson, Arizona where the source is a hammer blow against the mine wall. The resulting vibrations are recorded along a horizontal line of vertical-component receivers located about 30 m above on the surface. The goal is to image the source location from traces recorded in the far-field of the source and assesses the possibility of sub-wavelength imaging of scatterers in the near-field of the source.

The recording array consists of 60 receivers along the ground surface with a receiver interval of 0.5 m and there are 25 shot positions with a horizontal shot spacing of 0.5 m inside the tunnel at a depth of 30 m deep. At each shot location, two different files are recorded: the first one consists of the single-stacked shot gather d($\mathbf{g}$,t|$\mathbf{s}$,0) in Equation (1) and the second file contains the extrapolation shot gathers d($\mathbf{g}$,t|$\mathbf{s}'$,0) for s,$\mathbf{s}' \in B_s$ and $\mathbf{g} \in B_g$, with 16 stacks per shot gather to increase the signal-to-noise ratio. The direct arrivals in the traces are first muted to give the scattered data, then the traces are low-pass filtered with a pass range of 10-80 Hz and a stop value of 130 Hz. The Abbe horizontal resolution limit is calculated to be approximately $\Delta x = \frac{\lambda_{min}}{2}$ = 9.5 m. Here, the estimated minimum wavelength is $\lambda_{min} = \frac{V_p}{Freq.} = \frac{1470}{76}$ = 19 m. Both P-wave seismic velocity and peak frequency values are estimated from the collected shot gathers.

To isolate the scattered events from the direct waves, the recorded traces are separated into early arrivals and later arrivals. We define the early arrivals as the common shot gather windowed about the

direct-waves, and define the remaining part as later scattered arrivals. Then, Equation (1) is used to calculate the TRM profiles for the full 60-trace data and the half-aperture data where only 30 traces located along the middle of the geophone line are used. In this case, the "extrapolator" is the recorded data d($\mathbf{g}$,t|$\mathbf{s'}$,0) for a shot at $\mathbf{s'}$ and receiver at $\mathbf{g}$, and the "scattered data" is the recorded shot gather d($\mathbf{g}$,t|$\mathbf{s}$,0) (after muting the direct arrivals) for a source at $\mathbf{s}$ and a geophone at $\mathbf{g}$. In practice, the TRM profile is computed according to Equation (1) by zero-lag correlation of the trace d($\mathbf{g}$,t|$\mathbf{s'}$,0) with the trace d($\mathbf{g}$,t|$\mathbf{s}$,0) and summing over geophone positions to get m($\mathbf{s'}$), the TRM profile for the actual source at $\mathbf{s}$. Implicit in this windowing is the assumption that the near-field scattered energy is reverberating between the mine tunnel and the scatterer so that it appears after the first arrival.

Figure 3a depicts the TRM profiles m^{dir}($\mathbf{s}$') and $m^{dir/2}$($\mathbf{s}$') calculated, respectively, from the direct waves recorded in the full-aperture and half-aperture of traces. In contrast, m^{scatt}($\mathbf{s}$') and $m^{scatt/2}$($\mathbf{s}$') denote, respectively, the TRM profiles calculated from the scattered energy in the full- and half-aperture of traces. Here, the trial sources at $\mathbf{s}$' are located in the tunnel.

If the horizontal spatial resolution limit is defined to be the width at half the maximum amplitude, then Figure 3a shows that 1) the horizontal spatial resolution limits of $\Delta x^{scatt} < 1$ m and $\Delta x^{scatt/2} < 1$ m are smaller than $\Delta x^{dir} \approx 3$ m and $\Delta x^{dir/2} \approx 4$ m and 2) if only direct arrivals are used, the horizontal resolution limit gets worse as the receiver aperture decreases. The above resolution limit for the scattered data is approximately $\frac{\lambda_{min}}{19}$ and is well below the Abbe limit of $\frac{\lambda_{min}}{2} = 9.5$ m.

The sub-wavelength resolution limit of $\Delta x^{scatt} < 1$ m is consistent with the possibility that evanescent energy from the hammer source converts to propagating waves at nearby sub-wavelength scatterers, is recorded by the farfield geophones, and is digitally refocused to the source location by the TRM operation. To qualitatively estimate the distribution of these sub-wavelength features, Figure 3b shows the TRM profiles at different source and trial image points. It is clear that the better resolved source point locations are around the (6.3,6.3), (8.1,8.1), and (10.5,10.5) locations. The location around (6,6) m is in the general vicinity of the tunnel's widening as seen in Figure 4, which is also characterized by a faulted zone and meter-sized inclusions.

Conclusions

A practical use of a SSTM might be to migrate evanescent energy in downhole VSP data to estimate the crack intensity along the borehole. Alternatively, an indirect imaging method is to examine the TRM profiles as illustrated in Figure 3. Broad smooth peaks in the TRM profiles indicate a negligible density of sub-wavelength cracks in the near field, while sharper peaks indicate a higher density. Similar to a spectroscope, the data can be low-pass filtered to extend the region of the near-field and assess its crack density. The SSTM can employ surface waves as the generators of evanescent energy, and use the scattered Rayleigh waves as a high-frequency indicator of near-surface velocity variations; moreover, Stonely waves in a borehole can be used for this purpose as well. Another potential application is to use earthquake recordings, e.g., US Array, on the surface to estimate the calibration Green's functions. These calibration Green's functions might then be used to estimate the TRM profiles along the fault plane.

References

Cao, W., Hanafy, Sh., Schuster, G.T., Zhan, G. And Boonyasiriwat, C. [2012] High-resolution and super-stacking of time reversal mirrors in locating seismic sources. Geophysical Prospecting, **60**, 1-17.

Fink, M. [2008] Time-reversal waves and super-resolution. Journal of Physics, Conference Series. **124**, 1-29.

Schuster, G.T., Hanafy, Sh., and HuangY. [2012] Seismic Scanning Tunneling Macroscope: Theory. 74th EAGE Conference & Exhibition, Extended Abstracts.
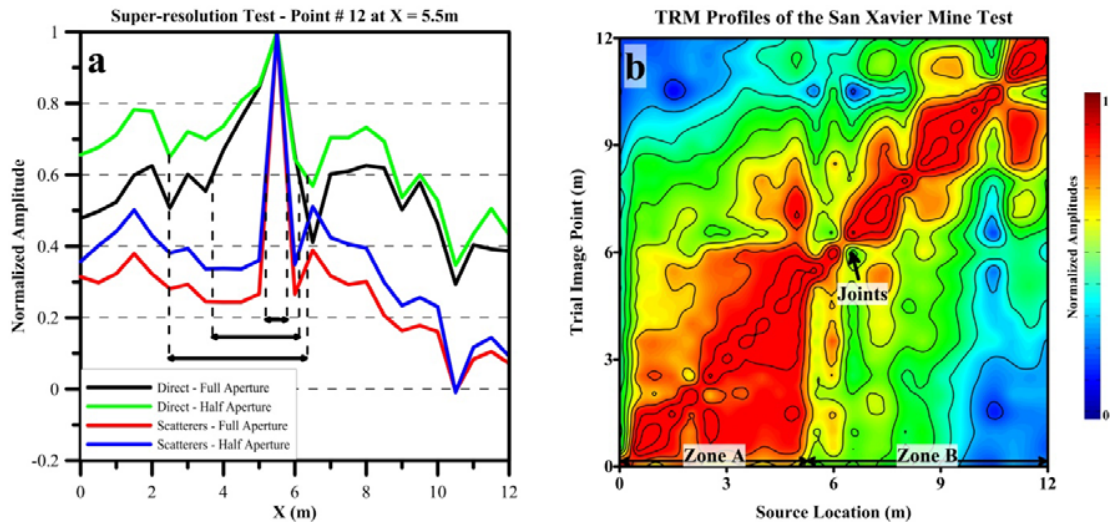
Figure 3 *a) TRM profiles m(x,z) calculated from traces that exclusively contained either direct waves (black and green) or scattered waves (red and blue). The source location is at x=5.5 m, and the TRM profile is computed for source points in the mine tunnel. b) TRM profiles for different shot positions plotted against trial image point locations. Varying the trial image point for source locations at 0< x <5 m yields broad red regions around the diagonal and indicate worse spatial resolution compared to the sources at around 6.3, 8.1 and 10.5 m.*

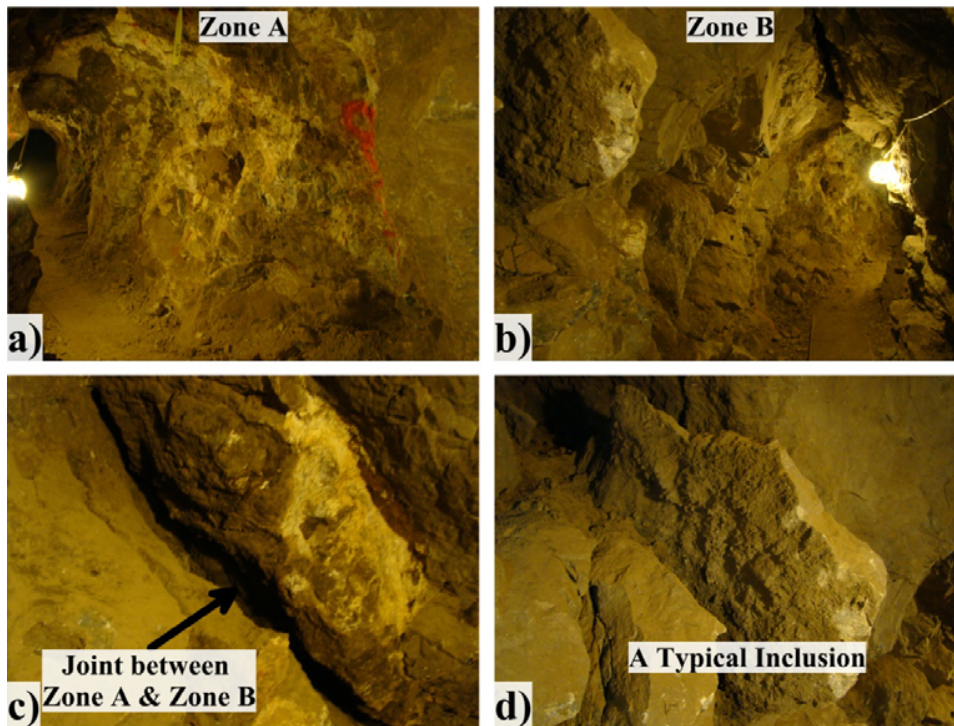## San Xavier Subsurface Tunnel

Figure 4 *Photos from inside the San Xavier Mine Tunnel. a) and b) are along the same wall, but a) shows mostly Zone A while b) shows Zone B. The red mark on the a) is approximately between Zones (A) and (B). c) Shows one of the joints that can be visually seen along the tunnel wall. d) is a typical inclusion about one meter in width.*